Global variables and correlations: Summary of the results presented at the Quark Matter 2012 conference

Boris Hippolyte[a], Dirk H. Rischke[b]

[a]*Institut Pluridisciplinaire Hubert Curien, Département de Recherches Subatomiques, 23 rue du Loess, F-67037 Strasbourg et Université de Strasbourg, France*
[b]*Institut für Theoretische Physik, Goethe University, Max-von-Laue-Str. 1, D-60438 Frankfurt am Main*

Abstract

In these proceedings, we highlight recent developments from both theory and experiment related to the global description of matter produced in ultra-relativistic heavy-ion collisions as presented during the Quark Matter 2012 conference.

1. Introduction

Describing the matter produced in ultra-relativistic heavy-ion collisions with a limited set of global variables is a tantalising task. In fact, the challenge is not only a description of the matter created under such extreme conditions but also an understanding of the details of its evolution. It is fair to say that stunning progress has occurred in the last couple of years, as it is reflected in the latest results presented during this edition of the Quark Matter conference. A significant fraction of the discussions focused on the shape of the initial energy density of the collision in terms of fluctuations. Such a picture is now constrained by extremely precise measurements of the azimuthal anisotropy of emitted particles as discussed in Sec. 2. A fairly detailed "standard model" for the dynamical evolution of a heavy-ion collision emerges and is explained in Sec. 3. Recently, lattice QCD calculations have made tremendous progress in eliminating systematic uncertainties. As explained in Sec. 4, various groups now agree on the value of the critical temperature for the chiral transition within systematic and statistical uncertainties, and on the value of the interaction measure at high temperature to within 25%. Section 5 is dedicated to recent experimental estimates of chemical and thermal freeze-out variables: statistical thermal analyses are performed on hadron abundances and comparisons are made for nuclei and hypernuclei as well. Baryon-to-meson ratios in the intermediate p_T region are studied at RHIC and LHC in order to investigate hadronisation mechanisms involving parton recombination. Blast-wave fits to hadron p_T-spectra are used to extract thermal freeze-out conditions as a function of collision centrality and beam energies. We conclude our review of global observables and fluctuations with an outlook towards further key questions that need to be addressed in the near future.

2. Constraints on fluid dynamics: azimuthal anisotropy

The fluid-dynamical description for the bulk dynamics of heavy-ion collisions received a tremendous boost in interest with the measurement of elliptic flow at RHIC, showing that fluid
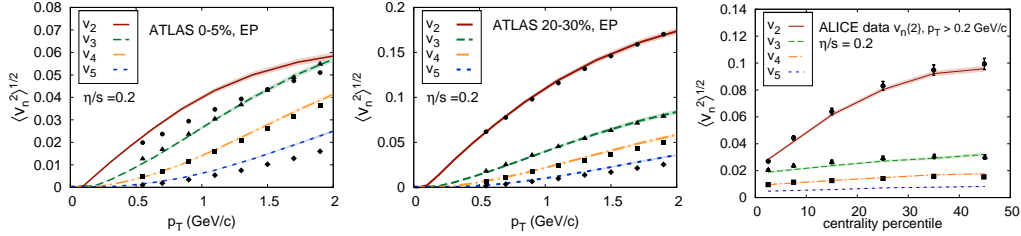
Figure 1: Harmonic flow coefficients for charged particles: left and middle panel as a function of p_T for two different centrality classes [6], right panel as a function of centrality percentile [5]. Calculations from Refs. [1, 7].

dynamics could quantitatively describe the collective flow of matter and coining the paradigm of the Quark-Gluon Plasma (QGP) being the "most perfect liquid" ever created. Later, fluctuation measurements were perceived as a handle on both initial state as well as transport properties of matter produced (first as a strongly interacting QGP – sQGP – and then as a hadron gas). Currently, we are at the crossroads where state-of-the-art modelling of initial conditions meets extremely precise experimental measurements of fluctuations. This is spectacularly illustrated by the presentation of B. Schenke with the "real (conference) time[1]" matching of the ATLAS event-by-event (EbyE) flow fluctuations for the anisotropic flow coefficients $v_{n=2,3,4}$ [2] by the Impact-Parameter Saturated (IP-Sat) Glasma modelling of the initial conditions [3], followed by 3+1–dimensional EbyE relativistic viscous fluid-dynamical evolution with MUSIC [4]. One of the striking features is that both p_T and centrality differential $v_{n=2,3,4,5}$ distributions from AT-LAS [2] and ALICE [5], respectively, are correctly reproduced with a single value of the shear viscosity over entropy density ratio $\eta/s = 0.2$ (see Fig. 1). Such a value is consistent with the quantification of the systematical uncertainties performed by M. Luzum and for which the "conservative" range of $0.07 \le \eta/s \le 0.43$ is obtained [8]. Nevertheless, it is a major achievement that IP-Sat Glasma initial conditions manage to reconcile v_2 and $v_{n\ge3}$ contrarily to MC-Glauber or MC-KLN initial energy density distributions for LHC energies. Moreover, with ultra-central collisions (2‰) recorded and selected by CMS [9] as well as with the studies of correlations between measured event-plane angles, one can expect new challenges for models and other insights into the fluctuations of the initial energy density. The main conclusions from the extraction of v_n with the Beam Energy Scan (BES) data at RHIC are similar but bring further constraints: when comparing to models, a low η/s is always favoured (i.e., close to 0.16) but the p_T-differential v_3 measured by STAR seems to increase progressively up to $\sim$ 30% with increasing beam energy $\sqrt{s_{NN}} = 11.5 \rightarrow 200$ GeV [10]. With the addition of particle identification ($\pi^\pm$, $K^\pm$, p, and $\overline{p}$) up to $p_T \simeq 4$ GeV/c at $\sqrt{s_{NN}} = 200$ GeV, PHENIX reports an ordering for $v_{n=3,4}$ with the same pattern than what is seen for v_2 and no beam energy dependence for p_T-differential $v_{n=3,4}$ for each particle species in a 20–60% centrality interval [11]. Although the analyses require more statistics, a significant effort is made by the experimental collaborations at RHIC and LHC to perform v_2 estimates with higher cumulants in order to isolate non-flow and fluctuation contributions. In parallel of the well-known fact that the p_T-integrated v_2 increases by $\sim$ 30% from top RHIC to LHC energies [12, 13, 14], it is underlined that the p_T-differential v_2 extracted with the 4-particle cumulant method stays close in the range $1 \le p_T \le 3$ GeV/c from lower BES RHIC to LHC

---

[1]The limited statistics at the time of the presentation was later improved, see Ref. [1].
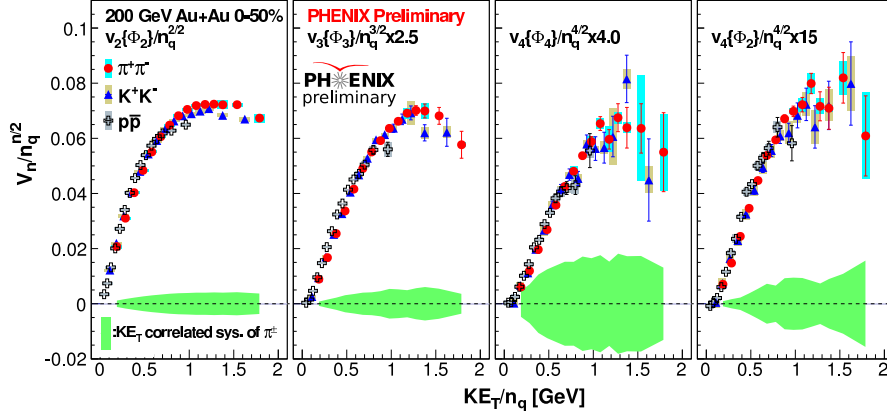
Figure 2: $v_n/n_q^{n/2}$ vs. KE_T/n_q with $n = 2$–4 (from left to right) for $\pi^\pm$, $K^\pm$, p+$\overline{p}$, in central (0–50%) Au–Au collisions at $\sqrt{s_{NN}} = 200$ GeV [11].

energies [15].

Concerning the LHC studies, it is also reported that (i) for all collision centralities, the measurements of integrated v_1 and v_3 do not change if one uses 4- or 6-particle cumulant methods (similarly to what was noticed for v_2); (ii) although v_3 shows also an increase with p_T, and then saturates around $p_T \simeq 3$ GeV/c, its centrality dependence is smaller than the one of v_2 (to be expected if initial density fluctuations are indeed at the origin of v_3) [16]. It is important to mention here the excellent agreement between different experiments when comparing v_2 obtained with the 4-particle cumulant method [14].

Several possibilities were investigated for finding a universal scaling for produced hadrons as a function of their number of constituent quarks (n_q) : (i) as shown in Fig. 2, PHENIX presented $v_n/n_q^{n/2}$ vs. KE_T/n_q for $\pi^\pm$, $K^\pm$, p+$\overline{p}$ which seems to hold for several harmonics (i.e., $n = 2$–4 for Au–Au collisions at $\sqrt{s_{NN}} = 200$ GeV) and several collision energies [11]; (ii) STAR reported that v_2/n_q vs. $(m_T - m_0)/n_q$ works for most identified particles and up to top RHIC energies except an intriguing 2-σ deviation for the ϕ meson at the lowest energies of $\sqrt{s_{NN}} = 7.7$ GeV and 11.5 GeV [15]; (iii) no scaling seems to hold up to LHC energies [16].

3. State-of-the-art modelling of heavy-ion collision dynamics

The "standard model" for the dynamical evolution of hot and dense strongly interacting matter created in ultra-relativistic heavy-ion collisions is the following: (i) individual parton-parton collisions copiously create gluons and quarks. The initial points of production are computed within various approaches. Some possibilities are the standard Glauber model for nucleon-nucleon collisions, the KLN model [17], or the IP-Glasma model [1, 3] which combines the Impact-Parameter Saturation (IP-Sat) model for the initial nuclear wave functions [18] with the classical Yang-Mills dynamics of the produced color fields ("Glasma") [19]. In a Monte-Carlo implementation of these models, initial conditions fluctuate from event to event. For an illustration, we show the transverse energy density profile at a time $\tau = 0.2$ fm/c after the collision in Fig. 3. The IP-Sat model shows fluctuations on the smallest scales, followed by the KLN
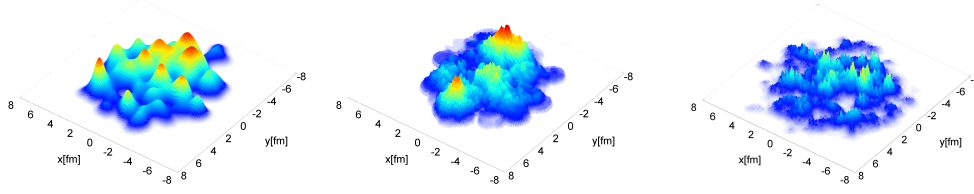
Figure 3: Initial conditions in the Glauber, the KLN, and the IP-Sat model, from Refs. [1, 7].

model. The Glauber model has the smoothest initial conditions, i.e., the smallest fluctuations. How these initial conditions evolve further and on which time scale thermalization is achieved is presently not clear. Calculations within ϕ^4 theory [20] show that actually thermalization (i.e., establishing an equation of state) is achieved prior to isotropization (i.e., equality of transverse and longitudinal pressure), cf. left panel of Fig. 4. This may necessitate the use of anisotropic fluid dynamics [21].

Commonly, one assumes a rather rapid approach to local thermodynamical equilibrium, so that fluid dynamics is applicable. The initial conditions for fluid dynamics are then specified on a hypersurface in space-time (commonly a constant proper time surface $\tau = \tau_0 = const.$). From then on, the evolution of the system is determined by the conservation laws for net-charge and energy-momentum,

$$\partial_\mu N^\mu = 0 \ , \quad \partial_\mu T^{\mu\nu} = 0 \ . \tag{1}$$

For a unique solution, causal and stable formulations of dissipative fluid dynamics require in addition dynamical equations for the dissipative components of N^μ and $T^{\mu\nu}$. For a systematic derivation of these equations from kinetic theory, see Ref. [22]. If the microscopic interaction rates drop below the macroscopic expansion rate of the fluid, a fluid cell will not be able to sustain (approximate) local thermodynamical equilibrium any longer; the cell "freezes out". This freeze-out process is commonly performed along a hypersurface of constant temperature [23]. How to compute the single-inclusive particle spectra in the presence of viscous terms was also reported at this conference [24]. The subsequent evolution of the system is either performed via a microscopic "afterburner" which takes into account elastic (and possibly inelastic) collisions between individual particles before they hit the detector (see, e.g. Refs. [25, 26]), or one simply assumes complete cessation of microscopic interactions. Then, one simply computes the single-inclusive particle spectra along the freeze-out hypersurface in order to compare with experimental data. Despite the apparent crudity of the underlying assumptions, the latter procedure is remarkably successful in reproducing the measured harmonic flow coefficients for charged particles, cf. Fig. 1 where they are shown for a calculation within relativistic dissipative fluid dynamics [1, 7] with IP-Glasma initial conditions and a constant shear viscosity-to-entropy density ratio of $\eta/s = 0.2$. One observes nearly perfect agreement for all flow coefficients for all centrality classes, except the most central one where the elliptic flow coefficient v_2 somewhat exceeds the experimental values.
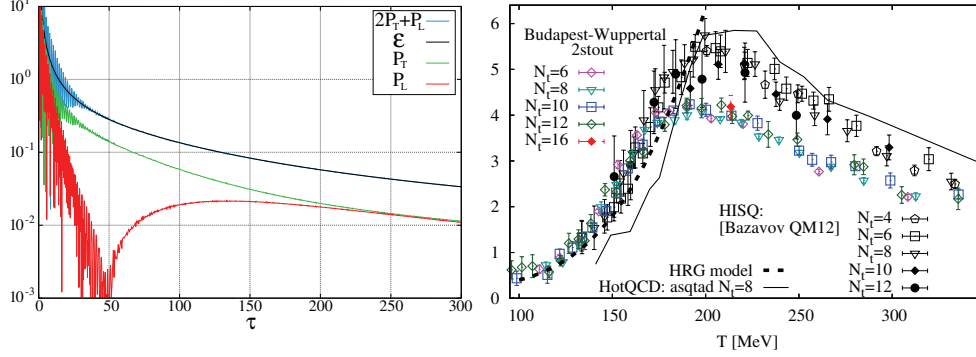
Figure 4: Left: evolution of various components of the energy-momentum tensor within ϕ^4 theory, from Ref. [20]. When $2P_T + P_L$ (blue) approaches the energy density (black), thermalization is achieved, while isotropization happens when the transverse (green) and longitudinal (red) pressure become degenerate. Right: the interaction measure $(\epsilon - 3p)/T^4$ from various lQCD calculations [29].

4. New lattice QCD results

As outlined in the former section, there remains a large uncertainty in the choice of initial conditions for fluid-dynamical calculations. Thus, there is little hope in being able to perform a reliable determination of the equation of state (and probably also of the transport coefficients) from experimental flow data. In this situation, lattice QCD (lQCD) remains the most important, and moreover quantitatively reliable, tool to provide microscopic input for fluid-dynamical calculations. There has been considerable progress in the past year: lQCD calculations from the HotQCD and Wuppertal-Budapest collaborations now agree on the value of (pseudo-)critical temperature for chiral symmetry restoration: $T_c = 154 \pm 8$ (stat.) ± 1 (sys.) MeV [27] vs. $T_c = 155 \pm 3$ (stat.) ± 3 (sys.) MeV [28]. Regarding the equation of state, one of the most important (systematic) uncertainties that remain to be resolved resides in the interaction measure. As can be seen from Fig. 4 (right), while the values of the HotQCD collaboration agree fairly well with those of the Wuppertal-Budapest collaboration below T_c, they are systematically larger by about 25% above T_c.

Another important input in dissipative fluid-dynamical calculations are the transport coefficients. One would hope that, in the future, lQCD calculations of these quantities reach a similar precision as those for the equation of state. Until then, one has to rely on more phenomenological approaches to extract values for η/s and the other coefficients, see e.g. [30, 31].

Correlations between, resp. fluctuations of, various quantities are an important tool to learn about critical behavior near phase transitions. This conference has seen a plethora of new data for these quantities. What is most striking is that lQCD calculations are now in the position to make firm predictions that can be directly compared to experimental data. Figure 5 shows $R_{31}^Q = \langle \delta N_Q^3 \rangle / \langle N_Q \rangle$ (left panel) and $R_{12}^Q = \langle N_Q \rangle / \langle \delta N_Q^2 \rangle$ (right panel), where N_Q is the net charge and $\delta N_Q = N_Q - \langle N_Q \rangle$ its deviation from its average [32]. R_{31}^Q is fairly insensitive to the value of the baryochemical potential μ_B, so it can serve as a thermometer to determine the (chemical) freeze-out temperature. Once the temperature has been extracted, R_{12}^Q, being fairly insensitive to temperature, can be used to extract the value of μ_B/T at (chemical) freeze-out.
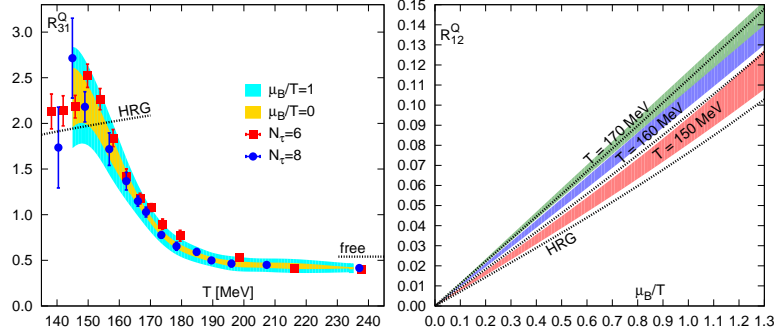
Figure 5: R^Q_{31} as function of T (left) and R^Q_{12} as function of μ_B/T (right), from Ref. [32].

5. Further constraints on chemical and thermal freeze-out

Once the QGP cools down and chemical freeze-out occurs, hadron abundances are very close to the ones recorded with the experimental setups. Statistical thermal model analyses of the hadron yields have been successfully describing the measurements on a large range of beam energies with few global variables only: the chemical freeze-out temperature T_{ch}, the baryo-chemical potential μ_B and the volume V of the fireball. The STAR analyses of BES data at RHIC offer the possibility to investigate not only the beam-energy but also the centrality dependence of these parameters [33]. For the lowest energies of $\sqrt{s_{NN}}$ = 11.5 and 7.7 GeV, the results of the fits for peripheral collisions seem to systematically depart[2] from the phenomenological description of 1 GeV per hadron [35]. The parameter extrapolation from RHIC to LHC energies is straightforward, since one expects T_{ch} to get closer to the deconfinement temperature T_c of lQCD and μ_B to vanish with increasing beam energy. However, some tension appears with the ALICE data analysis [36]: proton and anti-proton yields are low with respect to calculations for a temperature of T_{ch} = 164 MeV (see Fig. 6, left panel) which may reflect the presence of annihilation during the hadronic phase. The importance of corrections for feed-down and secondaries from interactions with the detector material is underlined together with the benefit of vertex detectors for this purpose [37]. Hypertriton and anti-hypertriton are measured not only at RHIC but also at the LHC. Using the BES data as well as the additional statistics of the 2012 run, the STAR Collaboration manages to obtain the excitation function of the $^3_\Lambda H + ^3_\Lambda \overline{H}$ p_T-spectra and refines the estimate of the lifetime τ with measurements in a larger decay length interval. A combined fit of 2010+2012 results gives: $\tau = 138 \pm^{23}_{60}$ ps [38]. Although ALICE extracts clear signals for $^3_\Lambda H$, $^3_\Lambda \overline{H}$ and $^4_\Lambda \overline{He}$, no H-dibaryon peak is observed and therefore, upper limits on the yields of this hypothetical particle are derived [39].

The observation of baryon/meson ratios at intermediate p_T being significantly higher for top RHIC energy Au–Au collisions as compared to pp triggered the development of models recombining quarks from the QGP phase to produce hadrons. STAR tried to isolate the possible onset of parton recombination looking at the hyperon production using the BES program and in particular the Ω/ϕ ratio vs. p_T: again, a difference seems to be seen for the lowest beam energies

---

[2]Both grand canonical and strangeness canonical ensembles are used within the THERMUS [34] code, which lead to opposite variations of the extracted T_{ch} parameter.
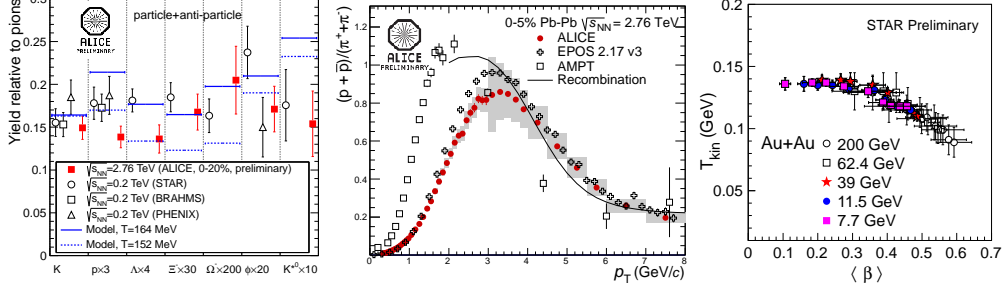
Figure 6: Left: comparison of hadron integrated yields to pion ratios at mid-rapidity for RHIC and LHC central collisions with thermal model predictions [36]. Center: comparison between the p/π ratio as a function of p_T for 0–5% central Pb–Pb collisions at $\sqrt{s_{NN}}$ = 2.76 TeV and several models [41]. Right: Evolution of T_{kin} vs. $\langle\beta_T\rangle$ extracted with simultaneous blast-wave fits to $\pi^\pm$, $K^\pm$, p, and $\bar{p}$ p_T-spectra for different centrality intervals and beam energies at RHIC [33].

$\sqrt{s_{NN}}$ = 11.5 GeV [40]. As illustrated by the p/π p_T-ratio as a function of the Pb–Pb collision centrality in Fig. 6 (center panel), the enhancement observed at RHIC still holds at LHC energies and the most central value (0–5%) is qualitatively compatible with several models using hadronisation mechanisms different from mere fragmentation [41]. A mapping of the kinetic freeze-out temperature T_{kin} vs. the mean transverse velocity $\langle\beta_T\rangle$ parameters is obtained performing blast-wave fits on $\pi^\pm$, $K^\pm$, p, and $\bar{p}$ p_T-spectra [33, 36]. Both beam energy and centrality dependences are investigated with collisions from $\sqrt{s_{NN}}$ = 7.7 GeV to 2.76 TeV. The evolution of the estimated radial flow is smooth with $\langle\beta_T\rangle$ increasing from ∼ 0.1 to 0.65 and simultaneously T_{kin} decreasing from ∼ 135 to below 100 MeV (see Fig. 6, right panel). For the most central collisions at the LHC, fluid-dynamical models are in general in good agreement with the identified p_T-spectra when a hadronic phase is included, in particular with antibaryon-baryon annihilation. The p_T-spectra corresponding to 100 events simulated with MUSIC [4]+UrQMD [42, 43] during the time of the conference are very close to the measurements [36].

6. Future prospects

In the very near future, we perceive it to be mandatory to scrutinize the new measurements and check the consistency of the experimental results. Models have to be validated in the energy range from $\sqrt{s}$ = 7.7 GeV up to 2.76 TeV. Then, systematic studies to further constrain the initial-state fluctuations are necessary. The hope is to get a better handle from detailed EbyE harmonic flow analyses, including event-plane angles. In particular, ultra-central events may serve as an interesting testing ground for models of the initial-state fluctuations.

On the theory side, further developments point into the direction of including thermal fluctuations into the fluid-dynamical modelling, see Ref. [44]. Of particular importance here seems to clarify how such fluctuations enter the dynamical equations of transient (second-order) fluid dynamics. Other interesting developments are the consistent description of the dynamics of the chiral order parameter within a fluid-dynamical framework [45]. Another interesting task for the future is the development of chiral anomalous fluid dynamics in order to assess the chiral magnetic effect [46] and the charge asymmetry observed by STAR [47] and ALICE [48].

Finally, explaining possible changes of hadron yields after chemical freeze-out (for instance,

7

due to baryon-antibaryon annihilation) and reconciling the statistical thermal model with data also seems to be an important task for future studies.

References

[1] B. Schenke *et al.*, these proceedings.
[2] J. Jia for the ATLAS Collaboration, these proceedings.
[3] B. Schenke, P. Tribedy and R. Venugopalan, Phys. Rev. Lett. **108**, 252301 (2012).
[4] S. Ryu *et al.*, these proceedings and references therein.
[5] K. Aamodt *et al.* (ALICE Collaboration) Phys. Rev. Lett. **107**, 032301 (2011).
[6] G. Aad *et al.* (ATLAS Collaboration), Phys. Rev. C **86**, 014907 (2012).
[7] C. Gale, S. Jeon, B. Schenke, P. Tribedy and R. Venugopalan, arXiv:1209.6330 [nucl-th];
[8] M. Luzum and J.-Y. Ollitrault, these proceedings.
[9] S. Tuo for the CMS Collaboration, these proceedings.
[10] Y. Pandit for the STAR Collaboration, these proceedings.
[11] Y. Gu for the PHENIX Collaboration, these proceedings.
[12] K. Aamodt *et al.* (ALICE Collaboration) Phys. Rev. Lett. **105**, 252302 (2010).
[13] S. Chatrchyan *et al.* (CMS Collaboration) arXiv:1204.1409 (2012).
[14] T. Bold for the ATLAS Collaboration, these proceedings.
[15] S. Shi for the STAR Collaboration, these proceedings.
[16] A. Bilandzic for the ALICE Collaboration, these proceedings.
[17] D. Kharzeev, E. Levin, M. Nardi, Nucl. Phys. A **747**, 609 (2005).
[18] J. Bartels, K. J. Golec-Biernat and H. Kowalski, Phys. Rev. D **66**, 014001 (2002); H. Kowalski and D. Teaney, Phys. Rev. D **68**, 114005 (2003).
[19] L. D. McLerran and R. Venugopalan, Phys. Rev. D **49**, 2233 (1994); D **49**, 3352 (1994); D **50**, 2225 (1994).
[20] K. Dusling, T. Epelbaum, F. Gelis and R. Venugopalan, Phys. Rev. D **86** 085040 (2012); R. Venugopalan, these proceedings.
[21] W. Florkowski, R. Maj, R. Ryblewski and M. Strickland, arXiv:1209.3671 [nucl-th]; W. Florkowski, these proceedings.
[22] G. S. Denicol, H. Niemi, E. Molnar and D. H. Rischke, Phys. Rev. D **85**, 114047 (2012).
[23] F. Cooper, G. Frye and E. Schonberg, Phys. Rev. D **11**, 192 (1975).
[24] G. S. Denicol, these proceedings.
[25] H. Song, S. A. Bass and U. Heinz, Phys. Rev. C **83**, 024912 (2011); H. Song, these proceedings.
[26] B. Schenke, S. Jeon and C. Gale, Phys. Rev. C **82**, 014903 (2010).
[27] A. Bazavov *et al.*, Phys. Rev. D **85**, 054503 (2012).
[28] S. Borsanyi *et al.* [Wuppertal-Budapest Collaboration], JHEP **1009**, 073 (2010).
[29] S. Borsanyi, arXiv:1210.6901 [hep-lat], these proceedings.
[30] P. Kovtun, G. D. Moore and P. Romatschke, Phys. Rev. D **84**, 025006 (2011); P. Romatschke, these proceedings.
[31] Y. Hidaka and R. D. Pisarski, Phys. Rev. D **81**, 076002 (2010); R. D. Pisarski, these proceedings.
[32] A. Bazavov *et al.*, arXiv:1208.1220 [hep-lat]; S. Mukherjee, these proceedings.
[33] S. Das for the STAR Collaboration, these proceedings.
[34] S. Wheaton *et al.*, Comput. Phys. Commun. **180**, 84 (2009).
[35] J. Cleymans and K. Redlich, Phys. Rev. Lett. **81**, 5284 (1998).
[36] L. Milano for the ALICE Collaboration, these proceedings.
[37] A. Andronic, P. Braun-Munzinger, K. Redlich and J. Stachel, these proceedings.
[38] Y. Zhu for the STAR Collaboration, these proceedings.
[39] B. Dönigus for the ALICE Collaboration, these proceedings.
[40] X. Zhang for the STAR Collaboration, these proceedings.
[41] A. Ortiz Vellasquez for the ALICE Collaboration, these proceedings.
[42] S. A. Bass *et al.*, Prog. Part. Nucl. Phys. **41**, 255 (1998).
[43] M. Bleicher *et al.*, J. Phys. **G25**, 1859 (1999).
[44] J. Kapusta, these proceedings; M. Stephanov, these proceedings.
[45] M. Nahrgang, these proceedings.
[46] D. E. Kharzeev, L. D. McLerran and H. J. Warringa, Nucl. Phys. A **803**, 227 (2008).
[47] G. Wang, these proceedings.
[48] Y. Hori, these proceedings.